Applied Magnetic Resonance 2, 179–202 (1991)

Applied Magnetic Resonance

Microwave and Optical Spectroscopy of Carotenoid Triplets in Light-Harvesting Complex LHC II of Spinach by Absorbance-Detected Magnetic Resonance

R.van der Vos[1], D.Carbonera[2] and A.J.Hoff[1]

[1]Department of Biophysics, Huygens Laboratory, Leiden University, Leiden, The Netherlands

[2]Department of Physical Chemistry, University of Padua, Padua, Italy

Received March 14, 1991

Abstract. Absorbance-detected magnetic resonance (ADMR) of the light-harvesting complex LHC II of spinach revealed two triplet contributions, having different D values, but equal E value ($|E| = 0.00379$ cm^{-1}). The two triplets are assigned to two of the three carotenoids present in LHC II: lutein ($|D| = 0.03853$ cm^{-1}) and neoxanthin ($|D| = 0.04003$ cm^{-1}). The ADMR-detected Triplet-minus-Singlet (T–S) optical difference spectrum of the carotenoid (Car) triplet transition of LHC II showed, apart from bands in the Car absorption region, a contribution in the chlorophyll (Chl) absorption region due to a change in interaction between lutein and Chl *a* at 670 nm, and neoxanthin and Chl *a* at 670 and 677 nm. From Linear Dichroic (LD-)ADMR-detected LD-(T–S) spectra we have determined that the triplet z-axis (which corresponds roughly to the polyenal axis) of lutein and neoxanthin makes an angle of 47° and 38° with the Q_y transition moment of their adjacent Chl *a* molecules, for the Chls absorbing at 670 and 677 nm, respectively. The T_z triplet magnetic transition moment of lutein is parallel to the lutein singlet and triplet absorptions, whereas the T_z axis of neoxanthin makes an angle of about 20 degrees with the optical transition moments of the carotenoid molecule. The major Chl *a* absorption bands of the optical absorption spectrum and the ADMR-detected T–S spectrum is best explained by assuming that all Chl *a* is present in dimers. It is proposed that a free Chl dimer absorbs at 664 and 670 nm, whereas a Chl dimer bound to a carotenoid absorbs at 670 and 677 nm.

1. Introduction

It is well known that carotenoids (Cars) present in photosynthetic systems have dual functions of light-harvesting and photo-protection [1,2]: they absorb light energy in the blue-green region and transfer it with high efficiency to Chls whereas a low-lying Car triplet state is formed by triplet transfer from the Chl

triplet. This prevents the formation of aggressive singlet oxygen. Not much is known about the mechanism of triplet-triplet transfer, geometry of the Car-Chl complex, etc., despite extensive studies carried out on Cars in reaction centers (RCs) and light-harvesting complexes of photosynthetic bacteria by optical time-resolved spectroscopy [3–6], electron paramagnetic resonance (EPR) [7–10] and recently Absorbance Detected Magnetic Resonance (ADMR) [11]. For higher plant systems even fewer studies have been done [12–14]. Recently, a triplet state in an isolated LHC II complex has been detected by EPR [15] and tentatively assigned to a Car. Here we extend this work with an ADMR study performed at 1.2 K of a LHC II-complex that was isolated in the same way as in [15]. We show that the EPR-detected triplet consists in fact of two different triplets with slightly different zero field splitting (zfs) parameters.

The triplet signals were assigned to lutein and neoxanthin with the aid of ADMR-detected Triplet-minus-Singlet (T–S) spectroscopy. In addition to the Car bands in the 400–550 nm region, the T–S spectrum showed interesting features in the 640–690 nm region, which are ascribed to Chl *a* molecules that interact with the Cars.

The geometry of the Car-Chl *a* complexes was partially elucidated with LD-ADMR.

2. Materials and Methods

2.1. Sample Preparation

LHC II-particles were prepared from spinach according to the method used by Bassi *et al.* [16] for Zea Mais L.. Photosystem (PS) II membranes were obtained according to the method of Berthold *et al.* [17], modified by Dunahay *et al.* [18].

PS II membranes were resuspended in 5 mM Hepes buffer pH 7.5, 1 mM EDTA, then solubilized in the presence of 1% DM (dodecyl maltoside) and centrifuged. Samples were loaded onto a 0.1 M sucrose gradient containing 0.06% DM. The LHC II band was dialized against PEG. The CP24 complex was completely absent in the preparation. The antenna complexes so obtained were diluted with 0.02 M Hepes pH 7.5, and glycerol was added to the sample in a ratio 2:1 (v/v). The OD of the sample was 0.4 (1 mm cuvet) at 670 nm.

We compared the ADMR signal of samples prepared with different concentrations of DM, and found that optimal signal intensity was obtained for a Chl:DM ratio of 1:40 (w/w). As a check we took the fluorescence and optical absorption spectra at 6 K and at room temperature, and compared them to the corresponding spectra of a sample which was not treated with DM. We observed a change in the intensity, but not in the shape, indicating that no significant structural changes had been induced [1].

For the stoichiometry of lutein, neoxanthin and violaxanthin we took the values of 1.75:1:0.44 from [15] obtained for a sample that was prepared in the same way as those for our ADMR experiments.

2.2. Experimental Set-Up

The ADMR set-up used for the ADMR experiments described in this work was completely rebuilt and differs somewhat from the set-up described in [19,20]. The microwave source was a HP8350B sweeper with plug-in HP8352A (0.01–8.4 GHz); its frequency was detected by a HP5350B counter. For experiments around 228 MHz the microwaves were amplified by an IFI wideband amplifier model M5580 (0.01–1000 MHz). Experiments with microwave frequencies above 1 GHz were done with a Varian travelling-wave tube amplifier VZL-6941 A1 (1–2 GHz). The steady-state ADMR experiments were performed with an output power of 1–3 W, whereas for transient ADMR at 228 MHz the full power of the IFI amplifier was used (70 W).

The microwave resonator was a helix for the experiments in which the microwaves were swept, and a loop-gap cavity [21,22] for ADMR-detected T–S spectroscopy. For ADMR at 228 MHz the minimal resonance frequency of the cavity described in [21,22] was lowered from 250 to 190 MHz by inserting a mica-plate ($\varepsilon_r \approx 8$) of about 30 μm thickness between the plates, and modifying the cavity by reducing the length of the loop compared to the length of the plates (see Fig.1).

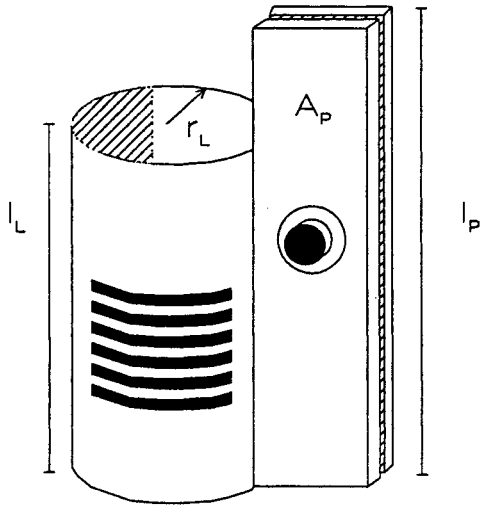

Fig.1. Schematic drawing of the modified loop-gap cavity. $l_{Loop} = 4.9$ cm, $l_{Plates} = 5.9$ cm, $r_{Loop} = 0.9$ cm, $A_{Plates} = 6$ cm^2.

The microwaves were amplitude modulated with a microwave switch operating at 315 Hz. For demodulation we used a Stanford Research Systems SR510 lock-in amplifier. For T−S spectroscopy at a fixed microwave frequency we scanned the wavelength in steps varying from 0.5 to 1.5 nm per point, stepping once every 1 to 3 s.

For transient ADMR experiments we used a EG&G 9650 pulse generator and a HP33190B microwave switch to generate the microwave pulses, and a Philips PM3320A digital oscilloscope to detect the transient signals.

The optical part of the set-up consisted of two lenses, one to focus the light on the sample, and one to focus the transmitted beam on the entrance slit of the Bausch & Lomb 825-1 monochromator with a B&L 825-2 grid of 1200 lines/mm having a blaze at 300 nm. The slitwidth varied from 1.5−2.5 mm for both the entrance and exit slit. The light was detected by a Peltier-cooled RCA30842 photodiode with a home-built preamplifier. For LD-ADMR-experiments the set-up was extended with a photoelastic modulator and an analyzer as described in [20,23]. We performed a LED-calibration as described in [23] to relate the isotropic and LD-(T−S) spectra. We can relate the ratio of the LD and the isotropic (T−S) signal, R, to the relative orientation of the optical transition moments with respect to the magnetic transition moment involved. The dependence of R on the angle of orientation is given in [23]. We used a perspex cuvet with dimensions 5×30×1 mm to hold the sample.

Sweeper, counter, lock-in amplifier, pulse generator and oscilloscope were all interfaced by an IEEE bus. The monochromator was interfaced by a home-built Local Measurement Computer. All data were acquired with a PC using a home-written measurement program.

3. Results

3.1. Optical Absorbance-Spectrum

The low-temperature optical absorbance spectrum of LHC II and its second derivative is shown in Fig.2. In the long-wavelength region only the Chls have absorption bands, the peak at 649 nm belonging to Chl *b* and the peaks at 664, 670 and 676 nm to Chl *a*. In the short-wavelength part of the spectrum the Chl and Car contributions overlap considerably, but it is still possible to recognize the Chl *a* maximum at 436 nm, the Chl *b* at 473 nm, and shoulders due to the Cars at 487 and 494 nm. We performed a Gaussian fit to the Chl region of the optical absorption spectrum. The parameters of the constituting bands are given in Table 1.

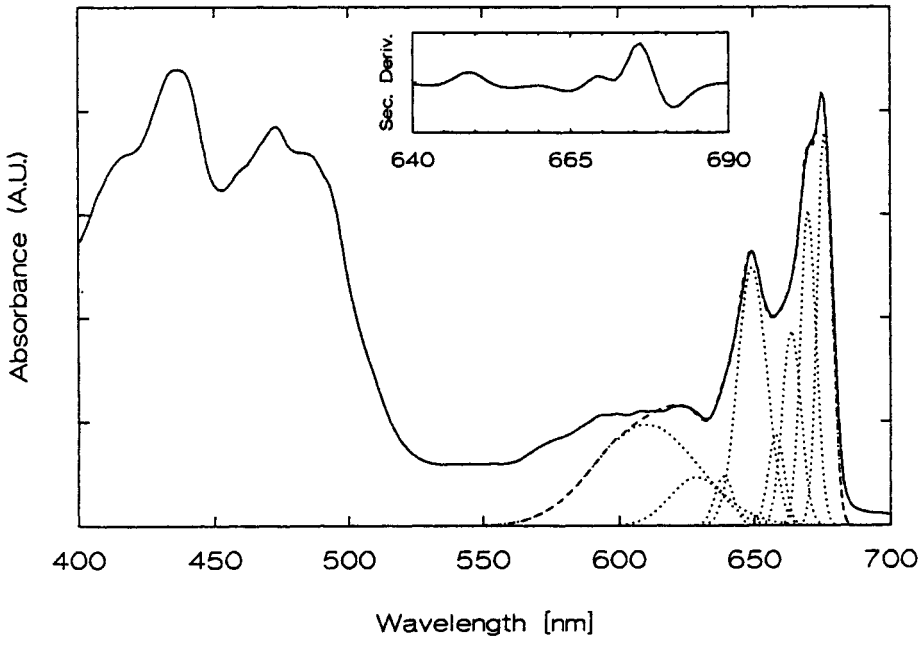

Fig.2. Absorption spectrum of the LHC II complex at 6 K: (---) – fit of the chlorophyll absorption region, (···) – constituting bands. Inset, second derivative. The spectrum was recorded with 1 nm resolution.

Table 1. Constituting bands of the Chl region (640–690 nm) of the optical absorption spectrum.

Center (nm) (±0.3 nm)	Width (cm^{-1}) (±5 cm^{-1})	Height (a.u.)
610.0	1180	0.24
628.5	590	0.11
638.5	200	0.11
649.0	300	0.60
658.0	160	0.21
664.0	180	0.45
670.0	140	0.73
676.0	140	0.93

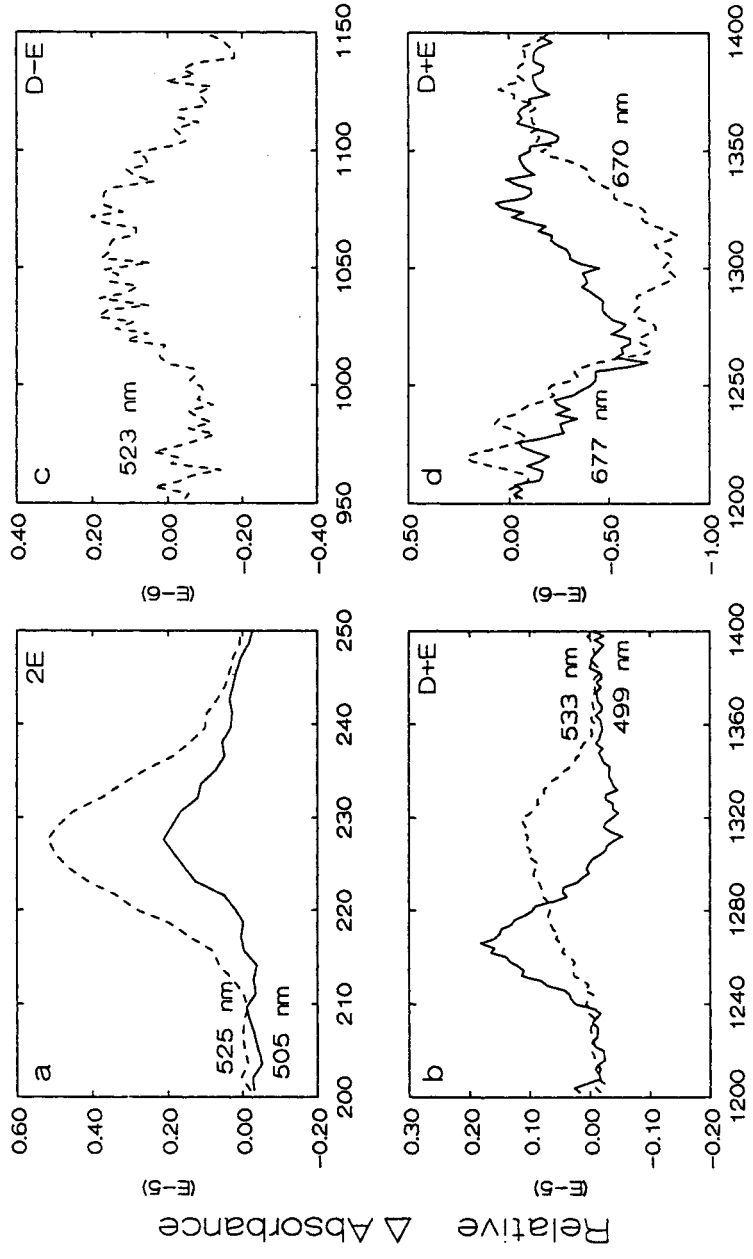

Fig.3. Microwave-swept ADMR spectra of the three triplet-transitions. **a** $2E$ transition, average of 9 scans, pre- and postfilter 1s: (——) – 525 nm, (---) – 505 nm. **b** $D+E$ transition, average of 9 scans, pre- and postfilter 1s: (——) – 533 nm, (---) – 499 nm. **c** $D-E$ transition, average of 25 scans, prefilter 3s, postfilter 1s, recorded at 523 nm. **d** $D+E$ transition, average of 16 scans, prefilter 3s, postfilter 1s: (——) – 677 nm, (---) – 670 nm.

3.2. ADMR

As stated before, we had to deal with two triplets that differed in their ADMR-detected T–S spectra. Both the ADMR lines and ADMR-detected T–S spectra overlapped considerably. To avoid this overlap as much as possible the ADMR lines were recorded at the edges of the bands of the ADMR-detected T–S spectra, and conversely the ADMR-detected T–S spectra were recorded at frequencies at which the triplets overlapped as little as possible.

3.3. Microwave-Swept Spectra

Figure 3a shows an ADMR transition at 228 MHz, whose width and intensity, but not frequency, depend on the detection wavelength. The frequency corresponds to that of the $2E$ transition of a Car [8,15]. In view of its wavelength independence, both major Cars, neoxanthin and lutein, contribute to the transition.

The $D+E$ transition shows different peak frequencies for the two detection wavelengths (Fig.3b). At 499 nm the maximum ADMR signal is at 1270 MHz, whereas at 533 nm the maximum is at 1310 MHz. From now on we will call the triplets the 1270 MHz triplet and the 1310 MHz triplet, respectively.

Figure 3d shows the lines of the $D+E$ transitions detected at the wavelengths corresponding to the bleachings observed in the 640–690 nm region. At 677 nm we observe a line similar to the one observed at 499 nm. The line observed at 670 nm, however, contains contributions of *both* triplets.

Deconvolution of the $D+E$ transition recorded at 533 nm reveals two contributions with their maxima at 1280 and 1315 MHz and a width of 40 MHz, which are present in a ratio of about 1:2. Both contributions are present in the same ratio in the $D+E$ transition recorded at 670 nm.

The $D-E$ transition (Fig.3c) gave rise to a very weak ADMR signal, which limited us to the ADMR line detected at 523 nm. The shape of this line is similar to the shape of the the $D+E$ transition detected at 523 nm (not shown).

3.4. Transient ADMR

We were only able to detect an ADMR transient at the $2E$ transition at 228 MHz using high light intensity, and a 5 μs microwave pulse, the width of which was limited by the weakness of the signal and the bandwidth of the photodiode preamplifier. Under these conditions we observed an increase in the transmittance, which decayed with a characteristic time of about 10 μs (data not shown).

3.5. Optical Triplet-Minus-Singlet Spectra

The ADMR-detected T−S spectrum shown in Fig.4 was detected at 228 MHz, the maximum of the $2E$ transition. In the Car absorption region bleachings are visible at 430, 457 and 492 nm. Positive contributions can be observed at 445, 475, 505 and 523 nm. In the Chl absorption region, we found two bleachings at 670 and 676 nm, and positive contributions at 650, 666 and 680 nm (inset Fig.4).

Led by the results of the experiments with swept microwaves near the $D+E$ transition, we recorded the ADMR-detected T−S spectra at fixed frequencies of 1257 and 1318 MHz, this with the intention to minimize the overlap between the two triplets. The results for the Car and the Chl region are shown in Figs.5a and 5b, respectively. Although the spectra are quite noisy, due to the low intensity of the ADMR signal at the frequency chosen, there is a clear difference between the two T−S spectra in both regions. Note, however, that in Figs.5a and 5b the spectra observed at 1257 MHz do not represent pure T−S spectra, due to only the 1270 MHz triplet, because of the overlap of the two ADMR transitions still present at the frequency chosen (Figs.3b and 3d). A full deconvolution is presented below; here we only note that the 1310 MHz triplet contributes to the triplet absorption maximum at 523 nm, and the bleachings at 500 and 670 nm, whereas the 1270 MHz triplet contributes to the triplet absorption at 505 nm, and to the bleachings at 490, 670 and 676 nm.

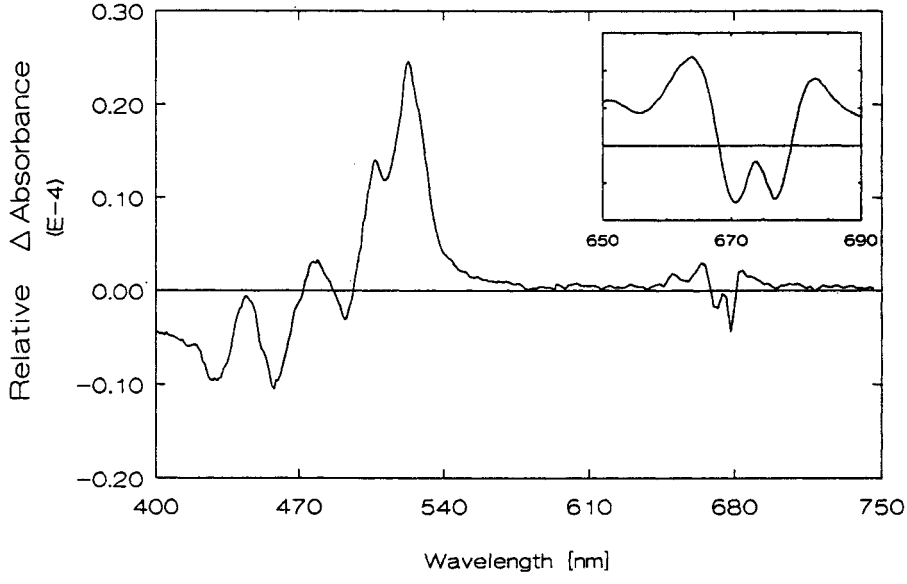

Fig.4. ADMR-detected T−S spectra from 400−750 nm, recorded at 228 MHz, average of 9 scans. Inset: Chl absorption region, average of 16 scans.

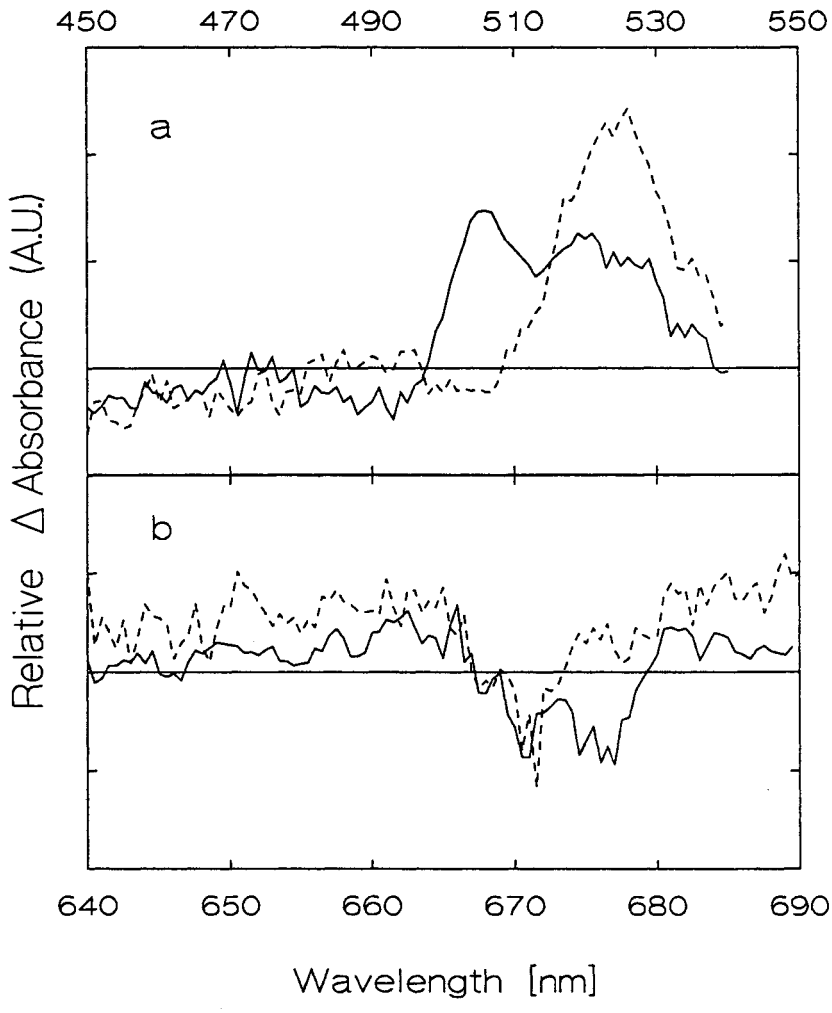

Fig.5. ADMR-detected T–S spectra recorded for excitation at the $D+E$ transitions at 1257 MHz (---) and 1318 MHz (——). Prefilter 3s, postfilter 1s. a The carotenoid region. Average of 9 scans. b The chlorophyll region. Average of 7 scans.

The positive band at 651 nm could be due to a change in Chl *b* absorption, induced by the presence of a Car triplet. Only one band was observed, possibly because the low intensity of the ADMR-signal in this region obscured other, weaker bands. Note that the amplitude of the 651 nm band to the T–S spectrum is a fraction of more than three smaller than the amplitude of the Chl *a* bands, whereas in the optical absorption spectrum the Chl *b* band is about a twofold more intense than the individual Chl *a* bands, so that the overall contribution to the T–S spectrum of Chl *b* is about a factor of six smaller than the Chl *a* contribution.

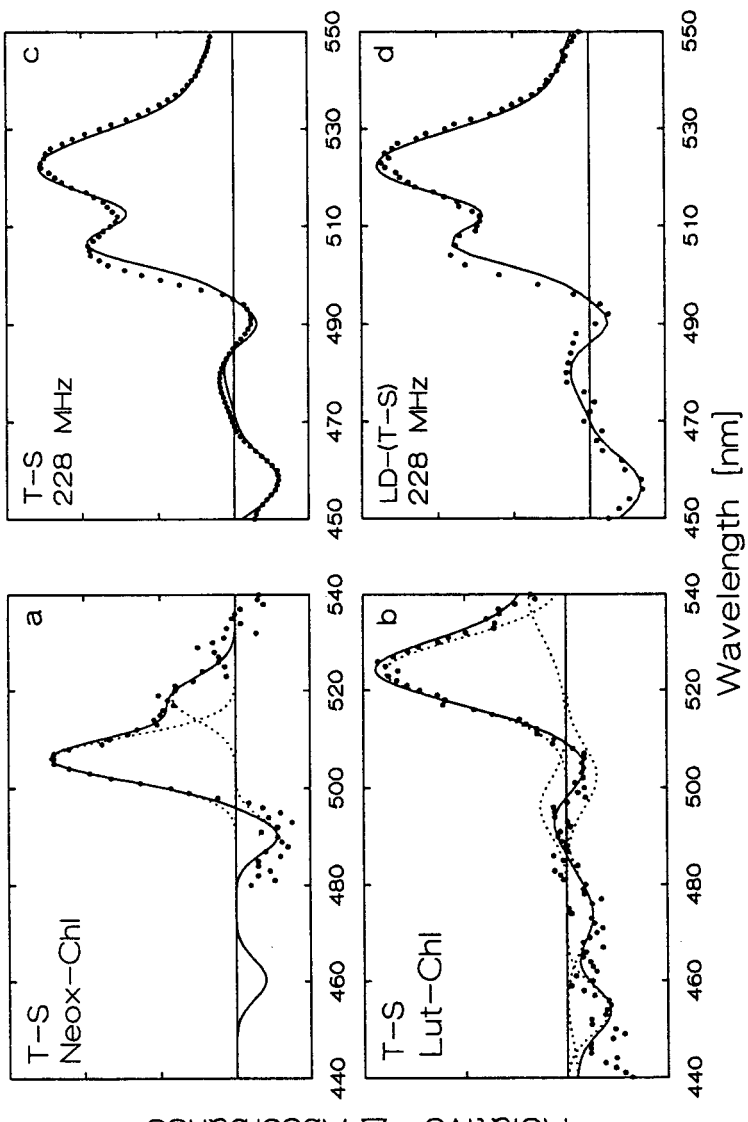

Fig.6. T–S spectra in the carotenoid absorption region. **a** "Pure" T–S spectrum of the neoxanthin-Chl complex: (●●●●) – spectrum determined as described in the text, (——) – fit, (····) – constituting bands. **b** "Pure" T–S spectrum of the lutein-Chl complex: (●●●●) – ADMR-detected T–S spectrum recorded at 1318 MHz (see Fig.5a), (——) – fit, (····) – constituting bands. **c** Reconstruction of the T–S spectrum recorded at 228 MHz with the two pure triplet contributions: (●●●●) – experimental spectrum (average of 16 scans), (——) – reconstruction. **d** Reconstruction of the LD-(T–S) spectrum recorded at the 2*E* transition (228 MHz): (●●●●) – experimental spectrum (prefilter 100 kHz lock-in amp. 30 ms, prefilter 315 Hz lock-in amp 3 s, postfilter 1 s, average of 16 scans), (——) – reconstruction.

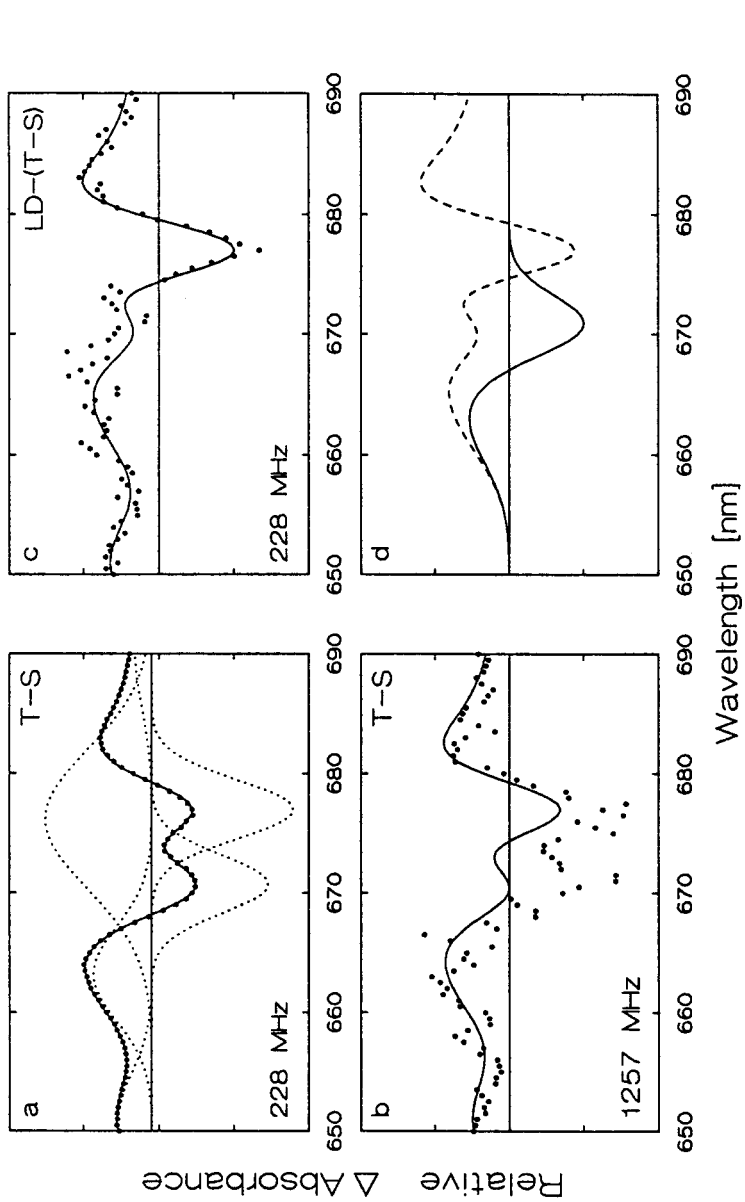

Fig.7. T–S spectra of the chlorophyll absorption region. **a** Fit of the T–S spectrum recorded at 228 MHz: (●●●●) – experimental spectrum, (——) – fit, (····) – constituting bands. **b** Fit of the T–S spectrum recorded at 1257 MHz: (●●●●) – experimental spectrum, average of 16 scans; (——) – fit, using the same bands as in Fig.7a, and spectral contributions as derived from the carotenoid absorption region. **c** Fit of the LD-(T–S) spectrum recorded at 228 MHz: (●●●●) – experimental spectrum, same conditions as in Fig.6d; (——) – fit, using the same bands as in Fig.7a. **d** The "pure" T–S spectra of the lutein-Chl complex (——) and the neoxanthin-Chl complex (----), calculated with the same bands as in Fig.7a, and a fraction x of 0.25.

3.6. LD-ADMR

We were able to record an LD-(T−S) spectrum only for the $2E$ transition at 228 MHz. The LD-ADMR signals of the other transitions were too weak to produce any meaningful results.

Figure 6d shows the LD-(T−S) spectrum for the Car region. The relative intensity of the Car bands is about the same compared to the isotropic spectrum, except for the triplet absorption at 523 nm, which shows a slight difference. In the Chl region (Fig.7c) we see that the relative intensity of the 670 and 676 nm bleachings has changed. This means that the bleachings at 670 and 676 nm are due to two different bands, and not to one broad bleaching with a narrow positive contribution in the center.

4. Discussion

4.1. ADMR Spectra

The zero field splitting parameters for the 1270 and 1310 MHz triplet are derived from the $2E$ and $D+E$ transitions. The value of $|D|$ is 0.03853 and 0.04003 cm^{-1} for the 1270 and 1310 MHz triplet, respectively. Both triplets have the same E value of $|E| = 0.00379$ cm^{-1}. These values are in good agreement with the D and E values found by EPR spectroscopy in [15], be it that there only one D value was found, situated in between the two values found here. This difference is due to the lower resolution of cw EPR spectroscopy.

4.2. Triplet Sublevel Populations

Pulse excitation at 228 MHz gives rise to a transient ADMR signal detected at 523 nm representing an increase of transmission. It follows that the microwave pulse decreases the triplet population. Because all ADMR transitions have the same sign, this conclusion holds for all three transitions of the triplet states involved. A possible sublevel scheme valid for both triplets is drawn in Fig.8, where the size of the circles qualitatively represents the size of the population of the different triplet sublevels. The scheme has been drawn for negative D, as from EPR spectroscopy on bacterial carotenoid-containing RCs it has been concluded that for bacterial carotenoids, and by inference for plant carotenoids, $D < 0$ [7].

The polarization found disagrees with the results derived from the EPR data in [15] where the population of the x-level dominates. This could be due to the

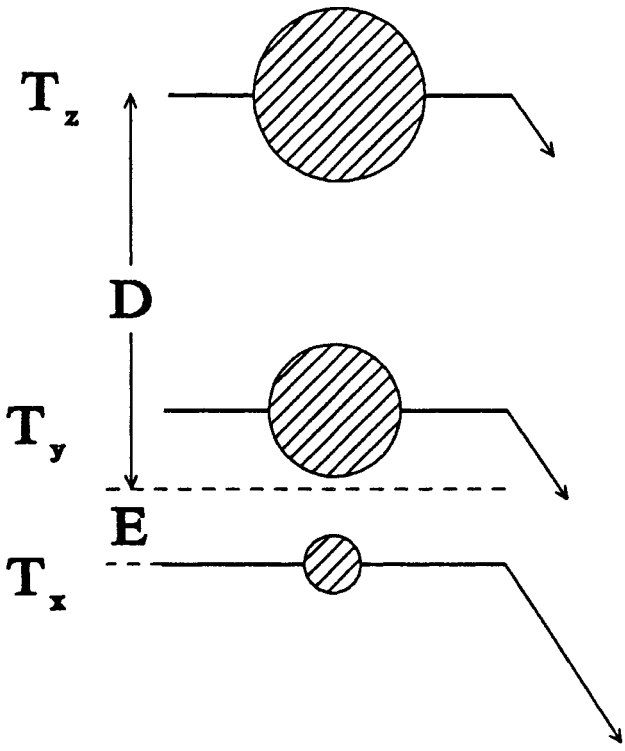

Fig.8. Schematic view of the distribution of the sublevel populations of the two carotenoid triplets.

different temperature at which the experiment was conducted. A temperature dependence of the ADMR signal was observed for carotenoids in bacterial antennas [11]. Another reason for this disagreement is perhaps that for the simulation of the EPR data only one triplet contribution was taken into account.

4.3. T–S Spectra in the Carotenoid Region

The T–S spectrum at 228 MHz is composed of two "pure" triplet contributions. From the microwave-swept ADMR data (Fig.3b) it is clear that only the 1310 MHz triplet contributes to the T–S spectrum recorded at 1318 MHz (Fig.6b). The T–S spectrum corresponding to the 1270 MHz triplet was calculated by determining the contribution of the 1310 MHz triplet to the T–S spectrum at 1257 MHz, and subtracting the contribution of the T–S spectrum measured at 1318 MHz from the spectrum observed at 1257 MHz. We normalized the spectrum on the areas of the triplet absorption bands. The T–S

spectrum corresponding to the 1270 MHz triplet thus obtained, is displayed in Fig.6a. It is seen that the 1310 MHz triplet contributes to the appearing bands at 525 and 540 nm and bleachings at 470 and 502 nm, whereas the 1270 MHz triplet contributes to two appearing bands at 505 and 516 nm, and a bleaching at 500 nm. For the 1270 MHz triplet we are not able to assign any bands below 480 nm, because of the low signal intensity.

As a check on the validity of the above-described decomposition of the T−S spectra in components due to the different triplet states, we reconstructed the T−S spectrum measured at 228 MHz with the two "pure" contributions. From Fig.6c it is seen that the reconstruction agrees quite well with the experimental spectrum for a ratio of the contribution of the pure T−S spectra corresponding to the 1270 and 1310 MHz triplet of 1:1.5. To obtain the stoichiometry of the compounds that give rise to the two triplets, we have to correct for their relative contribution to the $2E$ ADMR transition at the measuring frequency. This was determined from the area of the $2E$ transition measured at 505 nm (the 1270 MHz triplet) and 523 nm (the 1310 MHz triplet). The areas were taken proportional to the square root of the width of the lines (11 MHz at 505 nm and 15 MHz at 523 nm). This results in a correction factor of 1.18, so that the stoichiometry is 1:1.8. This agrees quite well with the stoichiometry 1:1.75 of neoxanthin and lutein in the LHC II complexes as determined by HPLC-analysis [15]. We therefore assign the 1270 MHz triplet to neoxanthin and the 1310 MHz triplet to lutein.

In the same way as we did for the $2E$ transition, we also determined the triplet abundances for the 1257 MHz $D+E$ transition and found a spectral contribution in the T−S spectrum of the Car region of 1.2:1 (1270 MHz triplet:1310 MHz triplet) and a triplet abundance of 1:2.0.

The above analysis rests on three assumptions. First we assumed that the steady state population difference between the x and y sublevels is similar for the two triplets. Since the lifetime of the slower decaying sublevel (which to first order determines Δn) is identical for the two triplets, and their populating characteristics will be similar (these depend on the geometry of the Chl-Car complex which is quite similar for the triplets considered, see below), this assumption seems to be warranted. The similar triplet abundances for both the 228 MHz $2E$ transition (1:1.8) and the 1257 MHz $D+E$ transition (1:2.0) support this assumption. Secondly, we have taken the same molar differential singlet-triplet extinction coefficient for lutein and neoxanthin. This seems to be reasonable as their singlet absorption coefficients are almost identical [27]. The third assumption concerns the neglectance of violaxanthin. Assuming that the Cars are solely excited to their triplet state by triplet-triplet transfer from Chl, we do not expect any contribution of violaxanthin to the ADMR-detected T−S spectrum, because it does not form a molecular complex with either Chl *a* or Chl *b* [27].

Table 2a summarizes the results of the fit of the Car region. The bands at 474 and 476 nm are ascribed to a change in Chl absorption, with likely also a contribution from the neoxanthin-Chl complex.

Table 2a. Constituting bands of the Car region (420–440 nm) of the T–S spectrum.

Center (nm) (±0.3 nm)	Width (cm^{-1}) (±5 cm^{-1})	Height (a.u.)	N/L[1]	Sign
445.0	760	0.06	n.a.[2]	–
454.0	500	0.23	L	–
460.5	450	0.14	N	–
474.0	680	0.14	L(N)	–
476.5	750	0.17	L(N)	+
490.5	360	0.20	N	–
496.0	540	0.14	L	+
502.5	580	0.17	L	–
506.0	410	0.86	N	+
518.5	390	0.30	N	+
524.0	570	1.00	L	+
540.5	770	0.21	L	+

[1] N – neoxanthin, L – lutein.
[2] n.a. – not assigned.

4.4. Chl a versus Chl b

It has been suggested [27] that the carotenoids in LHCs primarily bind to Chl *b*. The argument rests on the observation that in a Chl *b* lacking mutant of pea plants the yield of the 515 nm electrochromic shift signal of the carotenoids is significantly reduced. In addition, *in vitro* complexes of lutein with Chl *a* and Chl *b* show electrochromic shift maxima at 512 and 517 nm, respectively [27]. Evidently, the latter is somewhat closer to the *in vivo* 515 nm signal than the former. In contrast to the above contention we observe absorption difference signals in the Chl *b* region due to the formation of ^{3}Car that are ≦ 15 % of those in the Chl *a* absorption region. This indicates that Car-Chl *a* is a much tighter complex than the purported Car-Chl *b* complex. This is, of course, not really surprising. To act as a photoprotector, the Car molecule has to quench Chl triplet states. Since direct singlet-triplet transitions are spin-forbidden, so that triplet transfer by transition dipole interaction is very inefficient, this transfer predominantly takes place through exchange interaction, for which overlap of the donor and acceptor wavefunctions are required [27]. Even then, triplet transfer is usually much slower than singlet energy transfer, and occurs in about 12 ns [29]. Since excited Chl *b* loses its excitation very fast to Chl *a* by singlet

energy transfer (in 0.5±0.2 ps) [30], much faster than the time needed for intersystem crossing to the triplet state (a few ns), photoprotection by Car should predominantly occur in Car-Chl *a* complexes. Thus, although Car-Chl *b* complexes may exist for promoting singlet energy transfer from Car to Chl *b*, they play only a minor role in the sensitization of ^{3}Car and will be neglected in the discussion below.

4.5. T−S Spectra in the Chlorophyll Region

In order to resolve the absorption changes present in the Chl region, we performed a gaussian fit to the T−S and LD-(T−S) spectra recorded at 228 MHz, and to the T−S spectrum recorded at 1257 MHz simultaneously, taking into account the relative spectral contributions of the two triplets in the Car region. The values of the constituting bands are given in Table 2b. The Chl bleaching at 670 nm shows a large shift to 663 nm, which coincides with a band in the optical absorption spectrum. The Chl bleaching at 677 nm does not shift appreciably; it broadens and increases a little in dipolar strength.

The assignment of the bands to the two triplets discussed above is not trivial. From the *D*+*E* ADMR transition detected at 677 nm it directly follows that this bleaching is due to a neoxanthin-Chl complex. The *D*+*E* line detected at 670 nm, however, differs from those recorded at 533 and 499 nm, and in fact is composed of *overlapping* transitions of the two Car triplets. Comparing the shape of the *D*+*E* transitions recorded at 533 and 670 nm reveals that the two Car triplets contribute in the same ratio to the 670 nm bleaching as to the Car-spectral region, viz. neoxanthin:lutein equals 1.2:1.0. Thus, either all, or an equal fraction, *x*, of the lutein-Chl complex and the neoxanthin-Chl complex contributes to the 670 nm feature. Because the contribution of the 670 nm bleaching (to which both the lutein-Chl complex and the neoxanthin-Chl complex contribute) to the T−S spectrum observed at 228 MHz is smaller than that

Table 2b. Constituting bands of the Chl region (640−690 nm) of the T−S spectrum.

Center (nm)	Width (cm^{-1}) (±5 cm^{-1})	Height (a.u.)	N/L	Sign
651	210	4.8	n.a.	+
663.2	210	4.4	N/L	+
670.7	130	16.4	N/L	−
676.2	300	14.9	N	+
677.0	130	19.9	N	−
690.7	240	2.4	n.a.	+

of the 677 nm bleaching, to which only neoxanthin contributes, x is significantly smaller than one.

4.6. Relative Orientations Derived from LD-ADMR

The LD-ADMR experiments were performed at the $2E$ transition, between the T_x and the T_y sublevels. Thus, the orientation axis lies along the T_z axis, which presumably is close to the polyenal axis [31,32].

From the LD-(T–S) spectrum in the Car region we calculate, using the formalism outlined in [23], that for lutein the optical singlet-singlet and triplet-triplet transition moments are approximately parallel to the triplet magnetic transition moment (Table 3). From the high R-value for lutein (0.48) we conclude that we are far from power saturation (the microwave transition rate is much lower than the triplet decay rate). For neoxanthin we derive an angle of about 20 degrees.

The Chls absorbing at 670 and 677 nm differ in the orientation of the Q_y transition moments with respect to the triplet z-axis of the Cars. The 670 and 677 nm Chls make an angle of 47 and 37 degrees with this axis, respectively. The orientation of the Chls with respect to the z-axis shows a minor change ($\Delta R = 0.02 \pm 0.01$, which gives $\Delta\alpha = 1.6° \pm 0.7°$) when the Cars are in the triplet state, as evidenced by the slightly different dichroism for the corresponding positive and negative bands.

Table 3. Fit results LD-ADMR.

400–550 nm	$R(\alpha)$	α
Lutein-Chl	0.48	0–10°
Neoxanthin-Chl	0.41	20–22°
663.5 nm (+)	0.13	46°
670.3 nm (−)	0.10(0.20)	48° (41°)
676.3 nm (+)	0.23	38.5°
677.0 nm (−)	0.25 (0.50)	37° (0°)

4.7. Structure of the Carotenoid-Chlorophyll Complexes Chl a in LHC II

An acceptable model for the Car-Chl complexes involved should obey a number of boundary conditions imposed by our (and other) experimental results:

1. In the optical absorption spectrum the bands at 664, 670 and 676.5 nm contribute in a ratio of 1.5:2:3 (this work).
2. The stoichiometry of lutein and neoxanthin in LHC II is 1.75:1.0 [15].
3. The triplet population and decay rates of the lutein-Chl complex and the neoxanthin-Chl complex are about equal, otherwise the relative areas of the ADMR transitions of lutein and neoxanthin do not reflect their stoichiometry (see above).
4. The stoichiometry for Chl and the Chl-binding Cars lutein and neoxanthin is about 3:1 for LHC II complexes of lettuce [1].
5. The fractions x that give rise to the observed bleaching in the T−S spectrum at 670 nm are about equal for the lutein-Chl complex and the neoxanthin-Chl complex (this work).
6. The ratio of the spectral contributions of neoxanthin and lutein in the T−S spectrum detected at 228 MHz is 1:1.5, and at 1257 MHz 1.2:1 (this work).

Led by the two bleachings observed in the Chl region at 670 and 677 nm, and the fact that only one site of the Car is known to bind Chls [27], one is tempted to assign the two Chl bands to two different Car-Chl complexes. Assuming that both carotenoids form a complex with only one Chl, we propose that the fraction x of both Car-Chl complexes forms a complex with the Chl absorbing at 670 nm, whereas the Chl of the remaining fraction $1-x$ of the neoxanthin-Chl complex absorbs at 677 nm, and the remaining fraction of the lutein does not form a complex with Chl that gives rise to an ADMR-detectable T−S absorbance difference. From the fit of the T−S spectrum detected at 228 MHz and the spectral contributions of 1:1.5 for neoxanthin:lutein, we derive a fraction $x = 0.25$.

Apparently the remaining fraction $(1-x)$ of the lutein is sufficiently strongly bound to Chl for efficient triplet-triplet energy transfer, yet in such a way that the Chl absorption is insensitive to the electron state of the lutein. In the above calculation we have accounted for all Chl that absorbs at 670 nm. This leaves us with the question where the Chl of the lutein-Chl complex absorbs that does not contribute to the T−S spectrum of the complex. From the optical absorption spectrum we derive three possibilities: the missing Chl of the lutein-Chl complex can absorb at 664, 670, or 677 nm. If an equal fraction x of both the lutein-Chl complex and the neoxanthin-Chl complex contributes to the 670 nm bleaching band, and the remaining fraction $1-x$ of lutein-Chl to the 664 nm and that of neoxanthin-Chl to the 677 nm absorption band, we can calculate the ratio of the optical dipole strengths of the three absorption bands that is

needed to accommodate the measured stoichiometry of lutein and neoxanthin (1.75:1.0) and the above-derived value of x (0.25). We then find a ratio of 5:3:3 for the optical dipole strengths of the 664, 670 and 677 nm bands. This ratio is not consistent with the ratio derived from the fit of the optical absorption spectrum, viz. 1.5:2:3.

If we assume that the "missing" lutein-Chl complex absorbs at 677 nm, then consistency with the optical absorption spectrum can be obtained. However, in that case we derive from the 670/677 dipole strength ratio (2:3) for x a value of 0.4, i.e., a fraction 0.4 of both Car-Chl complexes absorbs at 670 nm, whereas the remaining fraction absorbs at 677 nm. This value of x clearly does not agree with the value calculated from the T−S spectrum (0.25).

This leaves us the third possibility, viz. that all lutein and a fraction x of neoxanthin is bound to the 670 nm Chl and the remaining fraction $1-x$ of neoxanthin is bound to the 677 nm Chl. This means that all 664 nm Chl and part of the 677 nm Chl is not complexed to a Car ("free" Chl).

We can now use conditions 1, 2 and 5 to calculate the ratio Car:total Chl for two situations: (i) all Chl is present as monomers, part of which is bound to Car, (ii) all Chl is present as dimers, whose constituent Chls are partly complexed to Car. The result is, that for (i) the Car:total Chl ratio is 1:2.4, whereas for (ii) it is 2.9. Thus, when all the Chl *a* is organized as dimers, the Car-Chl stoichiometry is closer to the value found for lettuce LHC II [1] than if we assume Chl monomers.

We will show below that the dimer model explains the major Chl *a* bands of the optical absorption spectrum and the ADMR-detected T−S spectrum, and to some extent the (LD-)T−S and optical CD spectra.

4.8. The Car-Chl$_2$ Model

Consider two types of Chl *a* dimers: one is complexed with a Car, and one consists of "free" Chls. The Car-Chl$_2$ complex absorbs at 670 and 677 nm, whereas the free Chl dimer absorbs at 664 and 676 nm. Assuming that all Car present is functional, that is, complexed with a Chl dimer, and using the stoichiometry for Chl *a* and the Cars lutein and neoxanthin as derived by [1] for LHC II complexes isolated from lettuce, 3:1 (or 6:2), the ratio free Chl:complexed Chl:Car becomes 2:4:2. If one (monomeric) Chl equivalent has an optical strength of S, then the free Chl dimer will contribute to the absorption bands at 664 and 677 nm with an optical strength of $2S$, whereas the complexed Chl dimer will contribute to its absorption bands at 670 nm and 677 nm with an optical strength of $4S$. This results in a total contribution to the absorption spectrum of 664:670:677 of $2S$:$4S$:($2S$+$4S$), or 1:2:3. From our fit of the optical absorption spectrum (cf. Table 1) we calculated a ratio of 1.5:2:3, which is close to the value obtained above.

Two models with Chl dimers that satisfy conditions 1–6 and explain our experimental results can be devised: in model A the two Chls of the same dimer interact with the same Car molecule: the 670 nm Chl is the Chl that is actually complexed to the Car, which causes its initial absorption wavelength of 664 nm to shift to 670 nm, whereas the 677 nm Chl (of the same dimer) has a π-π interaction with the polyenal axis of the neoxanthin, and no interaction with the lutein. As this Chl shows no, or a small (<1.5 nm) shift upon Car-Chl_2 complex formation, the absorption shift from ≈ 664 to 677 nm is probably due to environmental effects. (It is difficult to assign the 664 and 677 nm bands to a pair of exciton bands, as then one expects both to shift upon exciting the bound Car to the triplet state.) The π-π interaction with the polyenal axis causes the broadening observed for the neoxanthin 677 nm band in the T–S spectrum, because the π-electron density of the Car becomes more diffuse when it is in the triplet state [33]. The absence of such a broadening for the lutein-Chl_2 complex can be explained by assuming that the geometry of the neoxanthin-Chl_{670} complex and the lutein-Chl_{670} complex is different, such that the polyenal chain of lutein is too far away from the 677 nm Chl to have a π-π interaction. Presumably, the difference in geometry is due to the different position of the binding hydroxyl group in neoxanthin and lutein with respect to the polyenal chain. This model is illustrated in Fig.9.

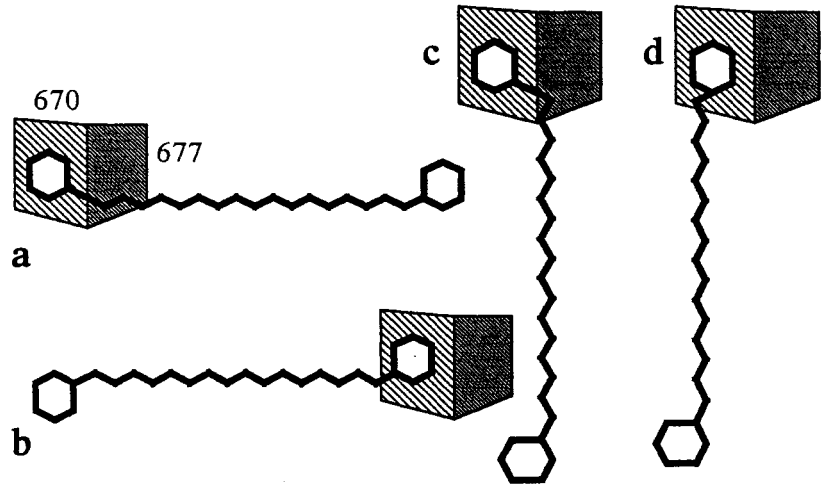

Fig.9. Possible conformations of the Car-Chl_2 complexes. The Q_y transition moment of the 670 nm Chl is situated such that it makes an angle of about 45° with the polyenal axis of the bound carotenoid (not indicated). **a** The neoxanthin-Chl_2 complex in the all-*trans* conformation. **b** The lutein-Chl_2 complex in the all-*trans* conformation. **c** The neoxanthin-Chl_2 complex in the 9-*cis* conformation. **d** The lutein-Chl_2 complex in the 9-*cis* conformation.

In the other model, B, two different kinds of Car-Chl_2 complexes are proposed: One complex, in which the 670 nm Chl is bound to the Car (neoxanthin or lutein) gives rise to the ADMR signal at 670 nm, and one complex, in which the 677 nm Chl is bound to the a fraction $1-x$ of the neoxanthin, gives rise to the broadening of the 677 nm band. In the latter complex, the 670 nm Chl is not bound to a Car and its absorption wavelength is shifted to 670 nm by environmental effects. In model B, each Car molecule interacts with only one Chl.

In both models we have to introduce a feature that explains why in a fraction x of the dimers the interaction of the 670 nm Chl with the Car is lost when the latter is in the triplet state, thus shifting the Chl absorbance back to 664 nm, whereas for the remaining fraction, $1-x$, the interaction persists, and no change in the T−S spectrum can be observed.

Above, we calculated a value for x of 0.25 for a fraction $1-x$ of neoxanthin having an interaction with 677 nm Chl. This represents the situation of model B. In model A, however, where one neoxanthin is complexed to both the 670 and the 677 nm Chl, also the fraction x that gives rise to a shift from 670 to 664 nm could be complexed to the 677 nm Chl and cause a broadening. In this case, we calculate a value for x of 0.32.

We can discriminate between the two possible values of x, by considering the Car absorption region. If a blue shift in the Chl region occurs due to a change in Chl-Car interaction, a corresponding red shift should be observed in the Car region. In the latter region we observe for both lutein and neoxanthin in addition to a big positive band, a smaller, red-shifted triplet absorption band, about 0.25 (lutein) to 0.33 (neoxanthin) the size of the first band.

We conclude that the absorption bands at 506 and 524 nm are due to neoxanthin and lutein, respectively, complexed to a Chl_2 in such a way that the Car-Chl_2 interaction does not change upon triplet formation (the fraction $1-x$). The 518.5 and 540.5 triplet absorption bands correspond to the "free" Car triplet absorption bands of neoxanthin and lutein, respectively (the fraction x observed in the Chl region). The fraction x calculated from the relative contributions of the triplet absorption bands is $0.25/1.25 = 0.2$ for lutein and $0.33/1.33 = 0.25$ for neoxanthin, in reasonable agreement with the value of x derived from models A and B under the assumption that the fraction x of the Car-Chl_{670} complexes is not complexed to 677 nm Chl.

The origin of the phenomenon that a fraction of the Car-Chl_2 complexes the Chl absorption is sensitive to the electronic state of the Car, is at present not clear. We may speculate that the fractions x and $1-x$ of the Car-Chl_2 complexes are due to different conformational states of the Cars involved. If the Cars are in the all-*trans* conformation, a change in bond order should occur near the center of the polyenal axis [34]. In the 9-*cis* or similar conformation, the change might occur closer to the binding site, and influence the binding energy of the Car, thus reducing the electronic interaction between the Chl and the Car in the triplet state. It is not unlikely that both Cars have the same prob-

ability to be in the 9-*cis* conformation, which explains the similar fractions x for both Cars. We have illustrated this schematically in Fig.9.

4.9. Chl-Car Binding

The two models presented above are consistent with the experimental data if it is assumed that the populating probabilities of the ^{3}Car triplet sublevels are the same for the lutein-Chl_2 and the neoxanthin-Chl_2 complexes. Since the triplets are formed by triplet-triplet transfer, this means that the projections of the triplet axes of ^{3}Chl onto those of ^{3}Car must be the same or similar for both types of Car. Thus, the orientation of the Car with respect to the Chl must be quite similar for the two Cars. This is reflected in Fig.9 for both the fractions x and $1-x$. Note that these two fractions may have different Δn, and therefore a different geometry, since the fractions x and $1-x$ are the same for the two Cars.

Note that the lutein and the neoxanthin behave similarly: both Car-Chl_2 complexes show the same shift from 670 to 664 nm, and also the triplet population and decay rates are about equal, because the lutein-neoxanthin stoichiometry can be retrieved from the triplet abundance. Thus, the conclusion of Sewe *et al.* [27] that neoxanthin forms a stronger complex with Chl than lutein is open to doubt.

4.10. Optical CD Spectroscopy

The maximum at 667 nm and the minimum at 670 nm as measured by CD spectroscopy of spinach chloroplast particles [35] and spinach LHC II particles [36] at 77 K can be well explained by the single contribution of the 676 nm band and the double contribution of the 664 and 670 nm absorption bands, which together yield a maximum at 667 nm.

4.11. Concluding Remarks

Very little is known of the molecular aspects of Car-Chl binding. Although the model of Car-Chl binding presented in this work is based on a number of novel spectroscopic results, it remains speculative. What is known on the precise structure of the bound Car comes mostly from resonant Resonance Raman (RR) studies, which indicate that the structure is highly twisted. In bacterial RCs the Car is almost certainly in the 15-*cis* configuration [37]; in the LHCs studied, the all-*trans* configurations seem to be preferred [38]. Two bacterial Car-containing RCs have been analyzed by X-rays, but the resolution is too low to confidently draw conclusions on isomerization, etc.

A key feature of our model is that part of the Cars in LHC II is in the 9-*cis* configuration, or a closely related conformer. This proposal is verifiable by RR spectroscopy on LHC II and appropriate model Cars *in vitro*, analogous to the work of Koyama *et al.* [34,38]. Time-resolved RR could shed more light on the intriguing finding that part of the neoxanthin forms a complex with Chl *a* that leads to line broadening in the triplet state. Another feature of our model is a different binding characteristic for the headgroup of neoxanthin compared to lutein, due to the different position of the OH end group. This aspect deserves further investigation, e.g. by electrochromic studies as in [27].

We believe that our conclusion that Cars bind predominantly to Chl *a* is firmly based. This, and the role of the protein in this specificity of binding could be further examined by investigations on molecular complexes of Chl *a*, Chl *b* and the various Cars by spectroscopic techniques as RR, (LD-)ADMR, time-resolved laser spectroscopy, etc.

Acknowledgements

We thank Drs. Stephan Otte and Jos van der Heiden for taking the absorption and fluorescence spectra at 6 K and at room temperature and Dr. F.Rigoni for the preparation of the LHC II complexes. We are indebted to Prof. G.Giacometti for his interest in this work. D.Carbonera is indebted to the Department of Biophysics of the Leiden University for its hospitality. This work was supported by the Netherlands Foundation for Chemical Research (SON), financed by the Netherlands Organization for Scientific Research (NWO).

References

[1] Siefermann-Harms, D.: Biochim. Biophys. Acta **811**, 325–355 (1985)
[2] Borland, C.F., Cogdell, R.J., Land, E.G., Truscott, T.G.: J. Photochem. Photobiol. **3**, 237–245 (1989)
[3] Bensasson, R., Land, E.J., Maudinas, B.: J. Photochem. Photobiol. **23**, 189–193 (1976)
[4] Renger, G., Wolff, Ch.: Biochim. Biophys. Acta **460**, 47–57 (1977)
[5] Cogdell, R.J., Land, E.G., Truscott, T.G.: Photochem. Photobiol. **38**, 723–725 (1983)
[6] Nuijs, A.M., van Grondelle, R., Laura, H., Joppe, P., van Bochove, C., Duysens, L.M.N.: Biochim. Biophys. Acta **810**, 94–105 (1985)
[7] Frank, H.A., Bolt, J.D., de B. Costa, S.M., Sauer, K.: J. Amer. Chem. Soc. **102**, 4893–4898 (1980)
[8] Frank, H.A., Machnicki, J., Felber, M.: Photochem. Photobiol. **35**, 713–718 (1982)
[9] Mc Gann, W.J., Frank, H.A.: Chem. Phys. Lett. **121**, 253–261 (1985)
[10] Frank, H.A., Chadwick, B.W., Oh, J.J., Gust, D., Moore, T.A., Liddell, P.A., Moore, A.L., Making, C.R., Cogdell, R.G.: Biochim. Biophys. Acta **892**, 253–263 (1987)
[11] Ullrich, J., Speer, R., Greis, J., von Schütz, J.U., Wolf, H.C., Cogdell, R.J.: Chem. Phys. Lett. **155**, 363–370 (1989)
[12] Gillbrö, T., Sundström, V., Sandström, A., Spangfort, M., Andersson, B.: FEBS Lett. **193**, 267–270 (1985)

[13] Nechustai, R., Thornber, J.P., Patterson, L.K., Fessenden, R.W., Levanon, H.: J. Phys. Chem. **92**, 1165–1168 (1988)
[14] Mathis, P., Schenck, C.C. in: IUPAC Carotenoid Chemistry and Biochemistry (Britton, G., Goodwin, T.W. eds.), pp.339–351, Pergamon Press: Oxford and New York 1982.
[15] Carbonera, D., Giacometti, G., Agostini, G., Toffoletti, A.: Gazetta Chim. It. **119**, 225–228 (1989)
[16] Bassi, R., Machold, O., Simpson, D.J.: Carlsberg Res. Commun. **50**, 145 (1985)
[17] Berthold, D.A., Babcock, G.T., Yocum, C.F.: FEBS Lett. **134**, 231 (1981)
[18] Dunahay, J.G., Staehelin, L.A., Seibert, M., Ogilvie, P.D., Berg, S.P.: Biochim. Biophys. Acta **764**, 179 (1984)
[19] den Blanken, H.J., Hoff, A.J.: Biochim. Biophys. Acta **681**, 365–374 (1982)
[20] den Blanken, H.J., Meiburg, R.F., Hoff, A.J.: Chem. Phys. Lett. **105**, 336–342 (1984)
[21] Froncisz, W., Hyde, J.S.: J. Magn. Res. **47**, 515–521 (1982)
[22] Hardy, W.N., Whitehead, L.A.: Rev. Sci. Instrum. **52**, 213–216 (1981)
[23] Lous, E.J., Hoff, A.J.: Proc. Natl. Acad. Sci. USA **84**, 6147–6151 (1987)
[24] Bensasson, R., Land, E.J., Maudinas, B.: Photochem. Photobiol. **23**, 189–193 (1976)
[25] Schenck, C.C., Mathis, P., Lutz, M.: Photochem. Photobiol. **39**, 407–417 (1984)
[26] Truscott, T.G., Land, E.J., Sykes, A.: Photochem. Photobiol. **17**, 43–51 (1973)
[27] Sewe, K.U., Reich, R.: Z. Naturforsch. **32c**, 161–171 (1977)
[28] Dexter, D.L.: J. Chem. Phys. **21**, 836–850 (1953)
[29] Kramer, H., Mathis, P.: Biochim. Biophys. Acta **593**, 319–329 (1980)
[30] Eads, D.D., Castner jr., E.W., Alberte, R.S., Mets, L., Fleming, G.R.: J. Phys. Chem. **93**, 8271–8275 (1989)
[31] Ros, M., Groenen, E.: Chem. Phys. Lett. **154**, 29–33 (1989)
[32] Frick, J., von Schütz, J.U., Wolf, H.C., Kothe, G.: Mol. Cryst. Liq. Cryst. **183**, 269–272 (1990)
[33] Lutz, M., Chinsky, L., Turpin, P.Y.: Photochem. Photobiol. **36**, 503–515 (1982)
[34] Hashimoto, H., Koyama, Y.: J. Phys. Chem. **92**, 2101–2108 (1988)
[35] Canaani, O.D., Sauer, K.: Biochim. Biophys. Acta **501**, 545–551 (1978)
[36] Hemelrijk, P.W., Kwa, S., Dekker, J., van Grondelle, R.: to be published.
[37] Lutz, M., Szponarski, W., Berger, G., Robert, B., Neumann, J.M.: Biochim. Biophys. Acta **894**, 423–433 (1987)
[38] Koyama, Y., Takatsuka, I., Kanaji, M., Tomimoto, K., Kito, M., Shimamura, T., Yamashita, J., Saiki, K., Tsukida, K.: Photochem. Photobiol. **51**, 119–128 (1990)

Author's address: Prof. A.J.Hoff, Department of Biophysics, Huygens Laboratory, Leiden University, P.O. Box 9604, 2300 RA Leiden, The Netherlands